

UDC 541.6:547.13:549.98

ON THE CHEMICAL BONDING FEATURES IN PALLADIUM CONTAINING COMPOUNDS: A COMBINED QTAIM/DFT TOPOLOGICAL ANALYSIS

L. Zeidabadinejad^{1,2}, M. Dehestani¹, S. Pourestarabadi¹

¹Department of Chemistry, Shahid Bahonar University of Kerman, Kerman, Iran

E-mail: S.Pourestarabadi@Gmail.com

²Young Researchers Society, Shahid Bahonar University of Kerman, Iran

Received October, 8, 2015

Revised — December, 3, 2015

Topological analyses of the electron density on N-benzoyl-L-pheylalanine and its palladium(II) complexes are carried out using the quantum theory of atoms in molecules (QTAIM) at the M06/6-31G(d) theoretical level. The topological parameters derived from the Bader theory are also analyzed; these are characteristics of Pd bond critical points and ring critical points. The calculated structural parameters are the highest occupied molecular orbital energy (E_{HOMO}), the lowest unoccupied molecular orbital energy (E_{LUMO}), the hardness (η), the softness (S), the absolute electronegativity (χ), the electrophilicity index (ω), and the fractions of electrons transferred (ΔN) from ethylenediamine, 2,2'-bipyridine and 1,10-phenanthroline complexes to N-benzoyl-L-pheylalanine. The numerous correlations and dependences between the energy terms of the symmetry adapted perturbation theory approach, geometrical, topological, and energy parameters are detected and described.

DOI: 10.15372/JSC20170307

Keywords: SAPT, QTAIM, charge transfer, the Bader theory.

INTRODUCTION

The important discovery of cisplatin heralded a new period of anticancer drug research based on metallopharmaceuticals [1]. Now cisplatin is very effective in the treatment of testicular and ovarian cancers and is also employed for treating bladder, cervical, head and neck, esophageal, and small cell lung cancer. Moreover, lobaplatin, nedaplatin, and heptaplatin have gained regional approval; a few platinum drugs continue to be evaluated in clinical studies. The main problems of current platinum drugs, including a limited range of cancers, acquired or intrinsic resistance, and severe side effects, prompted chemists to develop new metal anticancer drugs [2, 3]. However, some tumors such as non-small and colorectal cell lung cancers have intrinsic resistance to cisplatin, while others such as ovarian or small cell lung cancers develop acquired resistance after the initial treatment [4]. Owing to the thermodynamic and structural similarities between palladium(II) and platinum(II) complexes, there is increased interest in the study of palladium(II) derivatives as potential anticancer drugs [4—6]. For the first time, L.-W. Wang et al. synthesized palladium(II) complexes [Pd(en)A] (1), [Pd(bipy)A] (2), and [Pd(ph)A] (3) where A, en, bipy, and ph are N-benzoyl-L-pheylalanine, ethylenediamine, 2,2'-bipyridine, and 1,10-phenanthroline respectively [7]. It was established that the hydrolysis of the leaving ligands in palladium complexes was too rapid, therefore the complexes dissociated readily in the solution, leading to very reactive species unable to reach their pharmacological targets. This connotes that if anticancer palladium drugs can be developed, they must be stabilized by strongly coordinated nitrogen ligands and suitable leaving ligands. Phen and bipy or their derivatives have been used

to synthesize palladium anticancer complexes because **bipy** or **phen** have the capability to act as DNA intercalators [8, 9]. Many palladium complexes with aromatic N-containing ligands were shown to be effective against tumors. However, after more than 30 years of research since the discovery of the anti-tumor activity of cisplatin and cispalladium, no more than 30 compounds displaying sufficient pharmacological advantages relative to cisplatin and cispalladium have been found to be tested in clinical trials [10].

The theory that is able to identify the connectivity of bonds within molecules is QTAIM [11] which has also been applied for the characterization of long Pd—N and Pd—O bonds in palladium(II) complexes. Since the QTAIM approach provides much information about the nature of bondings, we have explored the topological properties of the electron density $\rho(\mathbf{r})$ and the Laplacian of the electron density $\nabla^2\rho(\mathbf{r})$ at various bond critical points (BCPs) to characterize the presence of possible open-shell and closed-shell interactions. The goal of this study is to apply density functional theory (DFT) calculations [12] and QTAIM theory [13] to quantitatively analyze the nature of bonds around palladium(II). We applied the charge analysis to investigate the properties of the bond and the electron charge transfer in palladium(II) complexes.

COMPUTATIONAL METHOD

All calculations, including optimizations and the NBO analysis were performed using the Gaussian 03 sets of code [14] at the M06/6-31G(*d*) level of theory without any symmetry restraints. Quantum chemical calculations of N-benzoyl-L-phenylalanine, ethylenediamine, 2,2'-bipyridine and 1,10-phenanthroline and palladium(II) complexes (**1**—**3**) were carried out with the M06/6-31G(*d*) basis set for C, H, N, O, Cl atoms and the LANL2DZ basis set for the palladium atoms.

QTAIM is also applied here, and the BCP and ring critical point (RCP) characteristics are analyzed in terms of the following properties: the electron density at the critical point, its Laplacian and the total electron energy density at the critical point. For the latter its components are also investigated: the potential electron energy density (V_b) and the kinetic electron energy density (G_b). The following relations are well-known if all terms are expressed in atomic units:

$$\frac{1}{4}\nabla^2\rho_b = 2G_b + V_b, \quad (1)$$

$$H_{e,b} = G_b + V_b. \quad (2)$$

The SAPT approach was applied to deepen the understanding of the nature of interactions [15] for complexes **1**—**3** and the MOLPRO package [16] was used to perform these calculations. SAPT is a well-established approach to calculate the interaction energy of two closed-shell moieties where the interaction energy is obtained directly as a sum of defined contributions. Thus, it is different from the commonly applied approaches where the binding energy is calculated as a difference between the energy of the complex and the sum of energies of monomers. In the SAPT approach the interaction energy consists of the following terms: the first-order electrostatics $E_{\text{elst}}^{(1)}$, second order induction $E_{\text{ind}}^{(2)}$, and dispersion $E_{\text{disp}}^{(2)}$ energies, and their exchange counterparts (first order exchange $E_{\text{exch}}^{(1)}$, second order exchange-induction $E_{\text{exch-ind}}^{(2)}$, and exchange-dispersion $E_{\text{exch-disp}}^{(2)}$). The SAPT method up to the second order gives the main part of the interaction energy. The SAPT2 interaction energy is calculated according to Eq. (3)

$$E_{\text{int}}^{\text{SAPT2}} = E_{\text{elst}}^{(1)} + E_{\text{int}}^{(2)} + E_{\text{disp}}^{(2)} + E_{\text{exch-int}}^{(2)} + E_{\text{exch-disp}}^{(2)} + \delta E_{\text{HF}}. \quad (3)$$

RESULTS AND DISCUSSION

Pd(**bipy**)Cl₂ crystallizes in the monoclinic space group *P2(1)/c*; selected bond distances and angles are listed in Table 1. The considered bond lengths and bond angles of the optimized structures of Pd(**ph**)Cl₂, Pd(**en**)Cl₂ and complexes **1**—**3** are also listed in Table 1 and all optimized structures are displayed in Fig. 1.

Table 1

Selected bond lengths (\AA) and angles (deg.) for the Pd(en)A, Pd(bipy)A, and Pd(ph)A complexes

Molecule	Bond length		Bond angle	
Pd(en)A	Pd—O1	1.8904	O1—Pd—N1	98.25
	Pd—N1	1.9708	O1—Pd—N2	175.21
Pd(bipy)A	Pd—O1	1.8932	O1—Pd—N1	95.36
		(1.9953) ^a		(94.18) ^a
Pd(ph)A	Pd—N1	1.9656	O1—Pd—N2	173.5
		(2.0095) ^a		(172.2) ^a
Pd(ph)A	Pd—O1	1.9300	O1—Pd—N1	95.98
	Pd—N1	1.9662	O1—Pd—N2	174.2
	Pd—N2	1.9726	O1—Pd—N3	84.39
	Pd—N3	1.9486	N1—Pd—N3	174.30
	Pd—N2	1.9701	O1—Pd—N3	83.75
		(2.019) ^a		(81.40) ^a
	Pd—N3	1.9576	N1—Pd—N3	176.27
		(2.0030) ^a		(175.30) ^a
Pd—N2	Pd—N2	1.9663	O1—Pd—N3	82.18
	Pd—N3	2.000	N1—Pd—N3	177.22

^a [7].

Relationships between the geometrical and topological parameters. The variety of atomic interactions can be approximately divided into shared (or covalent) interactions, intermediate (partially covalent) interactions, and closed-shell (van der Waals, ionic, metal, etc.) interactions [17–19]. The electron density feature at BCP is the fundamental difference between the two limiting extremes in the interactions, i.e., the closed-shell interactions and shared ones. In this way, the $H_{e,b} = G_b + V_b$ equation can be used to calculate the energy density, where V_b and G_b are the potential and kinetic energy densities, respectively [18, 19]. The shared interactions exhibit $\rho_b \geq 0.14$ a.u., $\nabla^2\rho_b < 0$, and $H_b < 0$, while closed-shell interactions show $\rho_b \leq 0.05$ a.u., $\nabla^2\rho_b > 0$, and $H_b > 0$. In the intermediate region $\nabla^2\rho(\mathbf{r}) > 0$ and $H(\mathbf{r}) < 0$. Table 2 shows the geometrical and topological parameters of RCPs in complexes 1–3. Briefly summarizing, a greater electron density at RCP of the intramolecular bond corresponds to a stronger interaction and a shorter bond length. Relatively negative $\nabla^2\rho_b$ values and positive $H_{e,b}$ values at *a*, *b*, and *c* bonds indicate that the electron density in the corresponding bonds in complex 3 is more than that in other complexes, so that the main nature of these bonds is partially covalent.

Local reactivity descriptors. The electron transition is due to the interaction between the highest occupied molecular orbital (HOMO) and the lowest unoccupied molecular orbital (LUMO) of reacting species, which is related to the frontier molecular orbital (FMO) theory of chemical reactivity [20]. E_{HOMO} measures the tendency towards the electron donation by a molecule; therefore, higher E_{HOMO} values indicate a better tendency towards the electron donation. E_{LUMO} indicates the ability of the molecule to accept electrons. The FMO diagram of A, Pd(en)Cl₂, Pd(bipy)Cl₂, and Pd(ph)Cl₂ is presented in Fig. 2.

The highest value E_{HOMO} , -2.88 eV in Pd(ph)Cl₂ indicates that the power attack in this molecule is more than in the other molecules. The E_{HOMO} values are in good agreement with the $\nabla^2\rho(\mathbf{r})$ values,

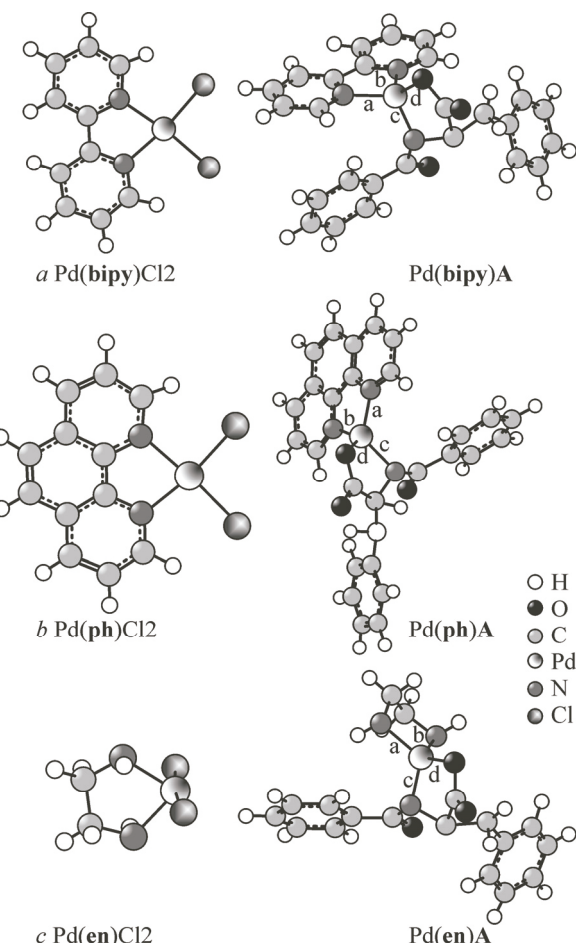


Fig. 1. Molecular structures of bipy and Pd(bipy)A (a), Ph and Pd(ph)A (b), and en and Pd(en)A (c)

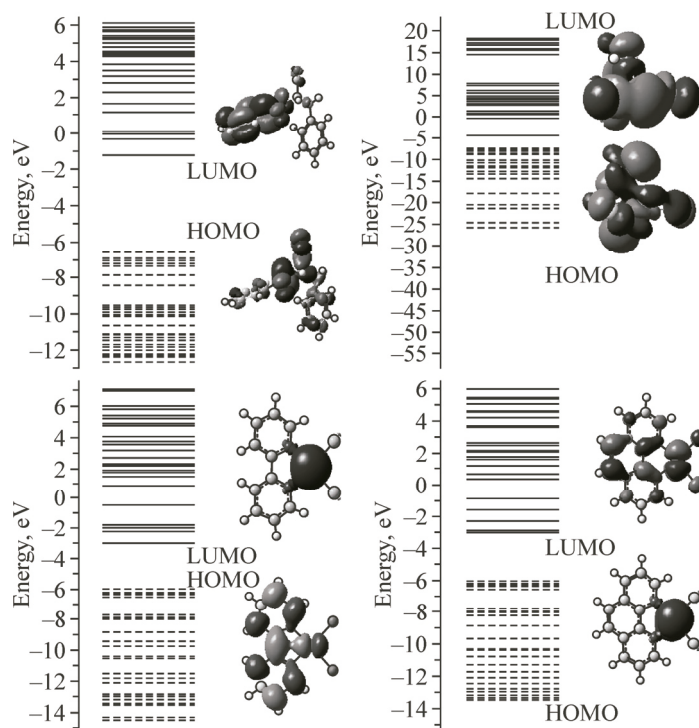


Fig. 2. Side view and molecular levels of **A**, $\text{Pd}(\text{en})\text{Cl}_2$, $\text{Pd}(\text{bipy})\text{Cl}_2$, and $\text{Pd}(\text{ph})\text{Cl}_2$

Table 2

*Topological properties of the charge density at BCP ($\rho(\mathbf{r})$, $\nabla^2\rho(\mathbf{r})$, and G_b , V_b and $H_{c,b}$; a.u.) of complexes **1—3***

Molecule	Bond	ρ_b	$\nabla^2\rho_b$	G_b	V_b	$H_{c,b}$
$\text{Pd}(\text{en})\text{A}$	a	0.12512	-0.11458	0.13287	-0.15115	0.01828
	b	0.12504	-0.12817	0.14650	-0.16482	0.01833
	c	0.12783	-0.14589	0.16491	-0.18393	0.01902
	d	0.13444	-0.23274	0.24437	-0.25601	0.01164
$\text{Pd}(\text{bipy})\text{A}$	a	0.11967	-0.17815	0.19037	-0.20259	0.01222
	b	0.30677	0.14846	0.49890	-0.54625	0.34736
	c	0.12386	-0.15133	0.16864	-0.18594	0.01730
	d	0.13368	-0.21255	0.22526	-0.23796	0.01271
$\text{Pd}(\text{ph})\text{A}$	a	0.12140	-0.18258	0.19514	-0.20768	0.01254
	b	0.12036	-0.17050	0.18263	-0.19477	0.01213
	c	0.11264	-0.15305	0.16511	-0.1716	0.01205
	d	0.12328	-0.20568	0.21542	-0.22516	0.00974

which can show that an increase in the HOMO energy can increase the electron density value at BCP and then increase the $\nabla^2\rho(\mathbf{r})$ value. As can be seen from Table 3, $\text{Pd}(\text{ph})\text{Cl}_2$ has the highest absolute values of E_{HOMO} and $\nabla^2\rho(\mathbf{r})$.

DFT has been found to be a successful theoretical method for the chemical reactivity and selectivity, in terms of popular qualitative chemical concepts such as χ , η , S , ω and local reactivity descriptors such as the Fukui function

$$\mu = \left[\frac{\partial E}{\partial N} \right]_{V(r)} = -\chi. \quad (4)$$

Table 3

Calculated E_{HOMO} , E_{LUMO} , ΔE , χ , μ , η , S , and ω for \mathbf{A} , $\text{Pd}(\mathbf{en})\text{Cl}_2$, $\text{Pd}(\mathbf{bipy})\text{Cl}_2$, $\text{Pd}(\mathbf{ph})\text{Cl}_2$, $\text{Pd}(\mathbf{en})\mathbf{A}$, $\text{Pd}(\mathbf{bipy})\mathbf{A}$, and $\text{Pd}(\mathbf{ph})\mathbf{A}$

Molecule	E_{HOMO} , a.u.	E_{LUMO} , a.u.	ΔE , a.u.	χ , eV	μ , eV	η , eV	S , eV	ω , eV
Pd(en)A	-0.18213	-0.13015	0.05198	0.156	-0.156	0.0259	0.0129	0.4690
Pd(bipy)A	-0.13518	-0.09543	0.03975	0.115	-0.115	0.0199	0.0099	0.3343
Pd(ph)A	-0.16675	-0.10133	0.06542	0.134	-0.134	0.0327	0.0163	0.2746
Pd(en)Cl ₂	-0.26973	-0.16553	0.1042	0.218	-0.218	0.0521	0.0260	0.4545
Pd(bipy)Cl ₂	-0.22087	-0.10885	0.11202	0.165	-0.165	0.0560	0.0280	0.2426
Pd(ph)Cl ₂	-0.2197	-0.10608	0.11362	0.163	-0.163	0.0568	0.0284	0.2334
A	-0.24237	-0.04316	0.19921	0.143	-0.143	0.0996	0.0498	0.1023

where μ , E , N , and $V(r)$ are the chemical potential, the total energy, the number of electrons, and the external potential of the system. The hardness has been defined as the second derivative of E with respect to N as the $V(r)$ property which measures both stability and reactivity of the molecule [21, 22]

$$\eta = \frac{1}{2} \left[\frac{\partial^2 E}{\partial N^2} \right]_{V(r)} = \frac{1}{2} \left[\frac{\partial \mu}{\partial N} \right], \quad (5)$$

where $V(r)$ and μ are the external and electronic chemical potentials, respectively.

According to Koopmans' theorem [12] for closed-shell molecules, the ionization potential (I) and the electron affinity (A) can be expressed in terms of E_{HOMO} and E_{LUMO} as follows:

$$I = -E_{\text{HOMO}}, \quad (6)$$

$$A = -E_{\text{LUMO}}. \quad (7)$$

When the I and A values are known, one can determine the absolute χ and η values through the following expression [23]:

$$\mu = -\frac{1}{2}(I + A), \quad (8)$$

$$\eta = \frac{1}{2}(I - A). \quad (9)$$

The softness is the inverse of the global hardness [24]

$$S = 1/\eta. \quad (10)$$

For a reaction of two molecules with different electronegativities the electronic flow occurs from the molecule with a lower electronegativity towards that with a higher value, until the chemical potentials are equal [25]. Therefore ΔN from the inhibitor molecule to the metallic atom was calculated according to the Pearson electronegativity scale [26]. The electrophilicity is a descriptor of the reactivity that allows a quantitative classification of the global electrophilic nature of a molecule within a relative scale. Parr et al. [22] have proposed the electrophilicity index as a measure of energy lowering due to the maximum electron flow between the donor and the acceptor. According to the definition, this index measures the tendency of chemical species to accept electrons. A more reactive nucleophile is characterized by lower μ and ω values, then a good electrophile is characterized by high μ and ω values. This new reactivity index measures the stabilization in energy when the system receives an additional electronic charge ΔN from the environment. They defined the electrophilicity index (ω) as follows:

$$\omega = \frac{\mu^2}{2\eta}. \quad (11)$$

Electrophilic charge transfer (ECT) [27] is explained as the difference between the ΔN_{\max} values of interacting molecules. We consider the approach of two Z (\mathbf{A}) and Y ($\text{Pd}(\mathbf{en})\text{Cl}_2$, $\text{Pd}(\mathbf{bipy})\text{Cl}_2$ and

Pd(**Ph**)Cl₂) molecules to each other, where two cases exist: (i) ECT > 0, charge flows from Y to Z and (ii) ECT < 0, charge flows from Z to Y. ECT is calculated by the following equation:

$$\text{ECT} = (\Delta N_{\max})_Z - (\Delta N_{\max})_Y, \quad (12)$$

where $(\Delta N_{\max})_Z = \mu_Z / \eta_Z$ and $(\Delta N_{\max})_Y = \mu_Y / \eta_Y$.

ECT is calculated as 2.744, 1.510, and 1.434 for complexes **1**—**3**, respectively. These results show that electrons are transferred from Pd(**en**)Cl₂, Pd(**bipy**)Cl₂, and Pd(**Ph**)Cl₂ to **A**. Therefore, **A** is treated as an electron acceptor and Pd(**en**)Cl₂, Pd(**bipy**)Cl₂, and Pd(**Ph**)Cl₂ are treated as electron donors. **A** exhibits the electrophilic behavior because the chemical potential value is low. As shown in Table 3, the high chemical potential and the low electrophilicity index for complexes **1**—**3** show their nucleophilic behavior.

The absolute hardness and softness are the important properties to measure the molecular stability and reactivity. A hard molecule has a large energy gap and a soft molecule has a small energy gap, it can be seen that the highest energy gap is related to the **A** molecule, since the charge transfer values show the direction of the charge from Pd(**en**)Cl₂, Pd(**bipy**)Cl₂, and Pd(**Ph**)Cl₂ to the **A** molecule.

In our study, the preferred site for the nucleophilic attack in the compound **A** is at O1 and H atoms. These results agree with the analysis of the LUMO densities, which also predicted these sites to be the most electron-deficient centers. The electrophilic attack would preferably occur at Pd atoms in Pd(**en**)Cl₂, Pd(**bipy**)Cl₂, and Pd(**Ph**)Cl₂. These results agree with the analysis of the HOMO densities, which also predicted these sites to be the most electron-rich centers. The parameters such as η , S , μ , A , I , χ , and ΔN confirm the direction of ECT from Pd(**en**)Cl₂, Pd(**bipy**)Cl₂, and Pd(**Ph**)Cl₂ to the ligand **A**.

SAPT calculations. SAPT applied here seems to be the proper approach to analyze the closed-shell interactions. It was mentioned previously that the nucleophilic attack of the palladium atom in **en**, **bipy**, and **ph** molecules on the **A** molecule leads to the formation of complexes **1**—**3**. Table 4 shows the SAPT2 interaction energy as well as the interaction energy terms in Eq. (3). If one considers the attractive (negative) terms of the interaction energy, the induction one $E_{\text{ind}}^{(2)}$ seems to be most important, followed by the electrostatic term $E_{\text{elst}}^{(1)}$ and the dispersive term. However, the induction and dispersive terms are strongly damped by their exchange counterparts $E_{\text{exch-ind}}^{(2)}$ and $E_{\text{exch-disp}}^{(2)}$, respectively. In the case of the induction interaction energy, it is reduced by 70—82 % while for the dispersive energy its reduction is 29—30 %. On the other hand, the first order electrostatic energy is outweighed by the first order exchange energy. Hence it shows the role of the induction energy in spite of the fact that the latter one is strongly reduced by its counterpart. There are other observations; the absolute dispersive energy values are greater for **ph** and **bipy** complexes than those for **en** complexes, even if the exchange counterpart of the dispersion energy is taken into account. However, all interaction energy terms are interrelated for the stronger interaction, and consequently, the shorter the intermolecular distance is, the greater the absolute values of all interaction energy terms. From a comparison of the dispersive energies with the total SAPT2 ones it follows that the dispersion contributes more to the stabilization energy for **ph** and **bipy** complexes than for **en** ones.

Table 4

SAPT interaction energies for Pd(**en**)**A**, Pd(**bipy**)**A**, and Pd(**ph**)**A**

Energy term, a.u.	Pd(en) A	Pd(bipy) A	Pd(ph) A	Energy term, a.u.	Pd(en) A	Pd(bipy) A	Pd(ph) A
$E_{\text{elst}}^{(1)}$	-9585.54	-10184.66	-10225.6	$E_{\text{exch-ind}}^{(2)}$	14696.23	15442.13	15627.33
$E_{\text{ind}}^{(2)}$	11227.12	11784.44	11926.80	$E_{\text{exch-disp}}^{(2)}$	959.7	1008.46	1020.56
$E_{\text{disp}}^{(2)}$	-18535.24	-19475.99	-19789.57	δE_{HF}	-1524.66	-1575.72	-1594.07
$E_{\text{exch}}^{(1)}$	-3216.07	-3404.57	-3445.39	$E_{\text{ind}}^{\text{SAPT2}}$	-5997.36	-6312.81	-6376.50

CONCLUSIONS

Complexes **1—3** and partially covalent interactions are considered here. It is found that for all interactions where the palladium atom acts as a nucleophile, we can state the relationship between the Pd—N distance and the Laplacian of the electron density at the corresponding BCP. It indicates the region of partially covalent bonds where the Laplacian is negative and the electron density is below 0.15 a.u. The electrophilic charge transfer confirms that electrons are transferred from $\text{Pd}(\text{en})\text{Cl}_2$, $\text{Pd}(\text{bipy})\text{Cl}_2$, and $\text{Pd}(\text{ph})\text{Cl}_2$ to the ligand **A**, so that the corresponding ligand is treated as an electron acceptor. The results of Fukui functions indicate the Pd atom attack of the ligand N atom.

The SAPT approach was also applied to analyze the interactions in the palladium complexes. It is found that the induction energy is the most important attractive interaction energy term for the complexes, followed by the electrostatic and dispersive terms. It means that for such strong interactions the electron density shift is very important for the complexation process, but the electrostatic interactions steer the arrangement of subunits in the complexes.

The authors express their great appreciation to the Department of Chemistry, Shahid Bahonar University of Kerman for supporting this investigation.

REFERENCES

1. *Fuertes M.A., Alonso C., Pérez J.M.* // Chem. Rev. – 2003. – **103**. – P. 645.
2. *Dempke W., Voigt W., Grothey A. et al.* // Anticancer Drugs. – 2000. – **11**. – P. 225.
3. *Wang D., Lippard S.J.* // Nat. Rev. Drug Discovery. – 2005. – **4**. – P. 307.
4. *Ray S., Mohan R., Singh J.K. et al.* // J. Am. Chem. Soc. – 2007. – **129**. – P. 15042.
5. *Ruiz J., Lorenzo J., Vicente C.* // Inorg. Chem. – 2008. – **47**. – P. 6990.
6. *Gao E.J., Zhu M.C., Huang Y. et al.* // Eur. J. Med. Chem. – 2010. – **45**. – P. 1034.
7. *Wang L.W., Liu S.Y., Wang J.J. et al.* // Synth. React. Inorg., Met.-Org., Nano-Met. Chem. – 2014. – **44**.
8. *Matilla A., Tercero J., Niclós-Gutiérrez J. et al.* // J. Inorg. Biochem. – 1994. – **55**. – P. 235.
9. *Bruijnincx P.C., Sadler P.J.* // Curr. Opin. Chem. Biol. – 2008. – **12**. – P. 197.
10. *Fuertes M., Castilla J., Alonso C. et al.* // Curr. Med. Chem. – 2003. – **10**. – P. 257.
11. *Bader R.F.W., Slee T.S., Cremer D. et al.* // J. Am. Chem. Soc. – 1983. – **105**. – P. 5061.
12. *Parr R.G., Yang R.G.P.W.* Density-functional theory of atoms and molecules. – UK, Oxford, 1989.
13. *Parr R.G., Gadem S.R., Bartolotti L.J.* // Proc. Natl. Acad. Sci. U. S. A. – 1979. – **76**. – P. 2522.
14. *Frisch M., Trucks G., Schlegel H. et al.* Gaussian 03. – Wallingford, CT, 2004.
15. *Jeziorski B., Moszynski R., Szalewicz K.* // Chem. Rev. – 1994. – **94**. – P. 1887.
16. *Werner H.J., Knowles P.J.* MOLPRO suite of programs, version 2012.
17. *Ranganathan A., Kulkarni G., Rao C.* // J. Phys. Chem. A. – 2003. – **107**. – P. 6073.
18. *Tang T.-H., Deretey E., Knak Jensen S. et al.* // Eur. Phys. J. D. – 2006. – **37**. – P. 217.
19. *Dominiak P.M., Grech E., Barr G. et al.* // Chem. – Eur. J. – 2003. – **9**. – P. 963.
20. *Parr R.G., Yang W.* // J. Am. Chem. Soc. – 1984. – **106**. – P. 4049.
21. *Geerlings P., De Proft F., Langenaeker W.* // Chem. Rev. – 2003. – **103**. – P. 1793.
22. *Parr R.G., Szentpaly L.V., Liu S.* // J. Am. Chem. Soc. – 1999. – **121**. – P. 1922.
23. *Pearson R.G.* // J. Am. Chem. Soc. – 1963. – **85**. – P. 3533.
24. *Lesar A., Milošev I.* // Chem. Phys. Lett. – 2009. – **483**. – P. 198.
25. *Martinez S.* // Mater. Chem. Phys. – 2003. – **77**. – P. 97.
26. *Pearson R.G.* // Inorg. Chem. – 1988. – **27**. – P. 734.
27. *Padmanabhan J., Parthasarathi R., Subramanian V. et al.* // J. Phys. Chem. A. – 2007. – **111**. – P. 1358.
28. *Senthilkumar K., Ramaswamy M., Kolandaivel P.* // Int. J. Quantum Chem. – 2001. – **81**. – P. 4.